



HAL
open science

A shear-induced network of aligned wormlike micelles in a sugar-based molecular gel. From gelation to biocompatibility assays

Juliette Fitremann, Barbara Lonetti, Emiliano Fratini, Isabelle Fabing, Bruno Payre, Christelle Boulé, Isabelle Loubinoux, Laurence Vaysse, Luis Oriol

► To cite this version:

Juliette Fitremann, Barbara Lonetti, Emiliano Fratini, Isabelle Fabing, Bruno Payre, et al.. A shear-induced network of aligned wormlike micelles in a sugar-based molecular gel. From gelation to biocompatibility assays. *Journal of Colloid and Interface Science*, 2017, 504, pp.721-730. 10.1016/j.jcis.2017.06.021 . hal-02060389

HAL Id: hal-02060389

<https://hal.science/hal-02060389>

Submitted on 25 May 2021

HAL is a multi-disciplinary open access archive for the deposit and dissemination of scientific research documents, whether they are published or not. The documents may come from teaching and research institutions in France or abroad, or from public or private research centers.

L'archive ouverte pluridisciplinaire **HAL**, est destinée au dépôt et à la diffusion de documents scientifiques de niveau recherche, publiés ou non, émanant des établissements d'enseignement et de recherche français ou étrangers, des laboratoires publics ou privés.

1 *This document is the author version of a work published in Journal of Colloid and Interface*
2 *Science, copyright ©Elsevier after peer review and technical editing by the publisher. The*
3 *final edited and published work is available at:*
4 <https://www.sciencedirect.com/science/article/abs/pii/S002197971730677X>

5 *Citation: Fitremann, J.; Lonetti, B.; Fratini, E.; Fabing, I.; Payré, B.; Boulé, C.; Loubinoux, I.;*
6 *Vaysse, L.; Oriol, L. A Shear-Induced Network of Aligned Wormlike Micelles in a Sugar-Based*
7 *Molecular Gel. From Gelation to Biocompatibility Assays. Journal of Colloid and Interface*
8 *Science* **2017**, *504*, 721–730. <https://doi.org/10.1016/j.jcis.2017.06.021>.

9

10 **A shear-induced network of aligned wormlike micelles in a sugar-based** 11 **molecular gel. From gelation to biocompatibility assays**

12 Juliette Fitremann^{*a}, Barbara Lonetti^a, Emiliano Fratini^b, Isabelle Fabing^c, Bruno Payré^d, Christelle Boulé^e,
13 Isabelle Loubinoux^f, Laurence Vaysse^f, Luis Oriol^g

14 *a CNRS - Université de Toulouse III Paul Sabatier, Laboratoire des Interactions Moléculaires et Réactivité Chimique et*
15 *Photochimique (IMRCP, UMR 5623), Bat 2R1, 118 Route de Narbonne, 31062 Toulouse Cedex 9, France.*

16 *b Department of Chemistry “Ugo Schiff” and CSGI, University of Florence, via della Lastruccia 3-Sesto Fiorentino, I-*
17 *50019, Florence, Italy.*

18 *c CNRS UMR 5068, LSPCMIB, Université de Toulouse, Université Paul Sabatier, 118 Route de Narbonne, 31062*
19 *Toulouse cedex 9, France.*

20 *d Centre de Microscopie Electronique Appliquée à la Biologie (CMEAB), Faculté de Médecine Rangueil, Université de*
21 *Toulouse III Paul Sabatier, Bâtiment A5, R.D.C., 133 Route de Narbonne, 31400 Toulouse, France.*

22 *e Université Claude Bernard UCBL Lyon1, Service de Prestations CTμ EZUS, Bâtiment Darwin B, 5 rue Raphaël*
23 *Dubois, 69622 Villeurbanne Cedex, France.*

24 *f TONIC, Toulouse NeuroImaging Center, Université de Toulouse, Inserm, UPS, France.*

25 *g Instituto de Ciencia de Materiales de Aragon (ICMA), Universidad de Zaragoza-CSIC, Dpto. Química Organica,*
26 *Facultad de Ciencias, Pedro Cerbuna 12, 50009 Zaragoza, Spain.*

27

28 A new low molecular weight hydrogelator with a saccharide (lactobionic) polar head linked by azide-
29 alkyne click chemistry was prepared in three steps. It was obtained in high purity without
30 chromatography, by phase separation and ultrafiltration of the aqueous gel. Gelation was not obtained
31 reproducibly by conventional heating-cooling cycles and instead was obtained by shearing the aqueous
32 solutions, from 2wt% to 0.25 wt%. This method of preparation favored the formation of a quite unusual
33 network of interconnected large but thin 2D-sheets (7 nm-thick) formed by the association side-by-side
34 of long and aligned 7 nm diameter wormlike micelles. It was responsible for the reproducible gelation
35 at the macroscopic scale. A second network made of helical fibres with a 10-13 nm diameter, more or
36 less intertwined was also formed but was scarcely able to sustain a macroscopic gel on its own. The gels
37 were analysed by TEM (Transmission Electronic Microscopy), cryo-TEM and SAXS (Small Angle X-
38 Ray Scattering). Molecular modelling was also used to highlight the possible conformations the
39 hydrogelator can take. The gels displayed a weak and reversible transition near 20°C, close to room
40 temperature, ascribed to the wormlike micelles 2D-sheets network. Heating over 30°C led to the loss of
41 the gel macroscopic integrity, but gel fragments were still observed in suspension. A second transition
42 near 50°C, ascribed to the network of helical fibers, finally dissolved completely these fragments. The

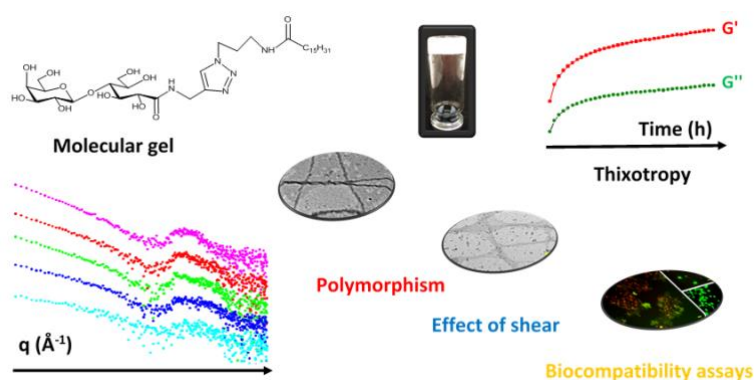
43 gels showed thixotropic behaviour, recovering slowly their initial elastic modulus, in few hours, after
44 injection through a needle. Stable gels were tested as scaffold for neural cell line culture, showing a
45 reduced biocompatibility. This new gelator is a clear illustration of how controlling the pathway was
46 critical for gel formation and how a new kind of self-assembly was obtained by shearing.

47

48 **Keywords:** supramolecular; gel; self-assembly; carbohydrate amphiphile; saccharide; triazole; fiber;
49 fibre; cylindrical micelle; shear; cell culture; biomaterial; LMWG; low molecular weight gelator.

50 **Electronic Supplementary Information:** Experimental section, extra electronic microscopy data,
51 HLPC-MS chromatograms, NMR spectra.

52 Graphical abstract



53

54

55 Introduction

56 Low molecular weight (LMW) hydrogelators provide an alternative family of gelling agents compared
57 with polymers, leading to soft materials with possible applications in the field of wet materials,
58 switchable gels, controlled release or uptake, cell culture. LMW gelators belong to different structural
59 families (peptides, cholesteryl, nucleobase or sugar amphiphiles, etc...) and the now quite large amount
60 of work done on these self-assembling molecules has been well reported in several reviews [1–21]. We
61 are more especially interested in sugar-derived molecular gelators (see the recent review on this family
62 of gelators and the following references for the most recent works [22–50]). Sugar gelators provide
63 generally a neutral hydrophilic polar head, with a low sensitivity to temperature changes on the contrary
64 to PEG amphiphiles. In the context of biological applications, carbohydrate derived hydrogels will
65 interact differently with biomolecules or cells compared with PEG or peptide derived gelators, notably
66 by mimicking to some extent the saccharidic components of the glycocalix, composed of glycoproteins
67 and glycolipids [22].

68 From a practical point of view, simple, rapid and cheap syntheses are essential when considering sugar-
69 based LMW hydrogelators applications. In former results, a family of hydrogelators based on a
70 disaccharide head has been described. It has been shown that the presence of a triazole linker enhanced
71 gelation, but the synthetic pathway consisted of six steps [23–26]. Other amphiphilic molecules with
72 close structures (namely, a sugar head, triazole linkers, and a fatty chain) have been described as well,
73 including hydrogelators [27–29], organogelators [30] and micelles [31–33], all of them involving also

74 protection-deprotection multistep synthesis and purification by chromatography. In this work, a new
 75 gelator inspired from these structures has been prepared with a simpler synthetic route with only three
 76 steps starting from lactobionic acid as the polar head (Scheme 1). Another important aspect in the field
 77 of LMW hydrogelators is to control in a precise manner the supramolecular structure sustaining the gel.
 78 In the case of very flexible molecules many conformations are possible. It can give rise to
 79 polymorphism. Polymorphism is the main cause for the lack of reproducible gelation [34–37].
 80 Accordingly, the importance of controlling the conditions of the self-assembly in order to reach a
 81 reproducible final state, with the related macroscopic properties, has been well pointed out in several
 82 papers. But it still remains underestimated, quite unexplored and not well controlled [38–42]. Compound
 83 **3** is a typical example of such a situation. Its gelation behaviour appeared more complex than expected
 84 and gave the opportunity to explore the effect of different pathways for the gel preparation. The self-
 85 assembled structures have been elucidated by electronic microscopy and Small Angle X-Ray Scattering
 86 (SAXS). The rheology and thermal transitions of the gel have also been studied. Finally, the results
 87 related to the use of these gels for cell culture are briefly discussed.

88

89 Results and discussion

90

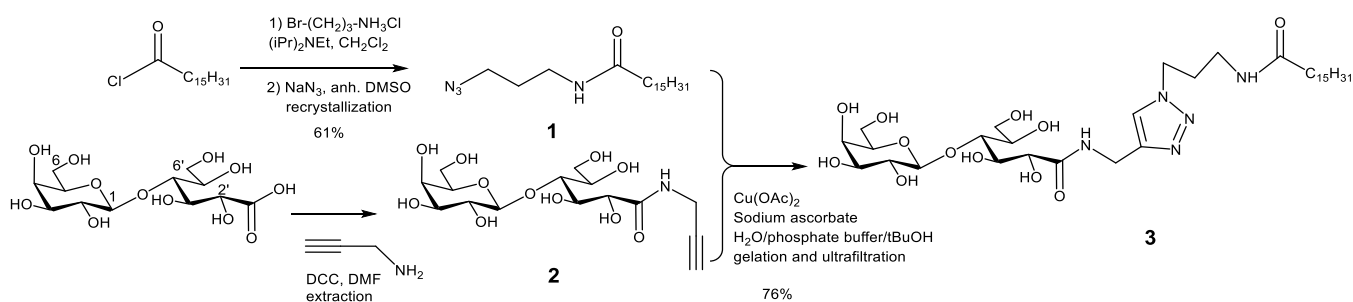
91 1. Preparation of the gelator

92

93 An easy access to the sugar based gelator **3** is represented in Scheme 1. The gelator was obtained
 94 in three synthetic steps and was purified without chromatography. The fatty chain **1** was purified
 95 by recrystallization (yield 60%) while the product **2** was obtained nearly pure by extraction and
 96 was used without further purification in the next step. After the azide-alkyne "click chemistry"
 97 step, leading to the compound **3**, the unreacted and sparingly soluble azide was discarded by
 98 centrifugation. The cleared and concentrated reaction medium was diluted in water and allowed
 99 to rest for several hours, until a gel was formed. The gel was purified by ultrafiltration or dialysis,
 100 removing water soluble by-products. Analysis of the filtrate showed that about 5% of the gelator
 101 went out through the membrane after four volumes and 24h of ultrafiltration, evidencing a low
 102 proportion of free molecules. A last step of filtration in methanol enabled to get rid of traces of
 103 the azide remaining after ultrafiltration. After this sequence, the gelator was pure (yield 76%,
 104 freeze-dried), according to NMR, HPLC-MS chromatograms (see Fig. SI-11-13). Residual
 105 copper was analysed and it did not exceed 300 ppm (0.3µg/mg) when ultrafiltration was
 106 performed in the presence of EDTA.

107

108



109

110 *Scheme 1. Synthetic scheme for the preparation of the gelator **3***

111 2. Gelation

112 Gelation of the gelator **3** was at first quite puzzling. The crude product coming directly from the
113 reaction mixture and diluted in water (after solvent removal) provided directly the hydrogel
114 within 24 hours of standing. Conversely, the purified and dried samples gave a non-reproducible
115 gelation behaviour. The usual method consisting in heating the solution until solubilisation
116 followed by cooling did not lead to reproducible gelation, whatever the concentration (from 0.1
117 to 2%wt). It has been checked that this effect was not the result of the degradation of the
118 molecule. It was still intact after heating for 4 hours at 60°C (see SI-12). Heating may favour a
119 change of intra or intermolecular bonding leading to insoluble aggregates instead of gel.
120 Concentrated samples at 2% usually provided gels but sometimes, viscous turbid solutions or
121 suspensions are obtained instead of gels. And conversely, it happened that very diluted samples
122 (0,3 to 0.1%) formed spontaneously gels, but in a non-reproducible manner (see SI-4).
123 Sonication did not help gelation (see SI-7), and the purification method did not appeared either
124 as the key parameter for gelation.

125
126 Finally, it was observed that shearing was a key factor for triggering the gelation reproducibly
127 for this compound. A reliable gelation procedure was then set up. A 2% suspension in water was
128 prepared and the hydration and solubilisation of the solid was allowed for few hours (2 to 24h).
129 It provided a heterogeneous suspension containing non-cohesive white cotton-like gels
130 fragments. The sample was then sheared through a needle until an homogeneous opalescent
131 solution was obtained. Finally, the sample was let resting for gelation at room temperature (20°C
132 or lower). A turbid gel, macroscopically homogenous was formed within c.a. 2 hours. It can be
133 turned upside down (Figure 6 and SI-1 "Gelation"). Additional cycles of shear/rest were
134 sometimes applied to improve gelation and homogeneity. The gel was also diluted stepwise up
135 to 0.25% by shearing, ranking the molecule among super-hydrogelators. Time also appeared as
136 a key factor for gelation, notably because of the solubilisation kinetics, but also because the gel
137 appeared to be thixotropic, but with a slow recovery (see section E-rheology).

138 The benefit of shear on gelation has already been observed in few examples of organogels
139 [43,44], hydrogels [45,46] and micellar solutions [47]. Shearing can affect, first, the distribution
140 of the aggregates in the solution and can help to get a more homogeneous distribution of the
141 growing self-assemblies. The shear can also affect the shape of the self-assemblies, by
142 lengthening the aggregates or even by changing the growth pathway and thus, the polymorph
143 formed, as it has been observed in the examples cited above. Shearing can also provide foam,
144 namely a large air-water interface on which the amphiphilic molecules can absorb and organize
145 before coalescence. The walls of the needle used to shear may also act as an interface for
146 organizing the molecules. In our case, the effect of shear on the gels of **3** will be discussed in the
147 light of SAXS, electronic microscopy and rheology (see section D).

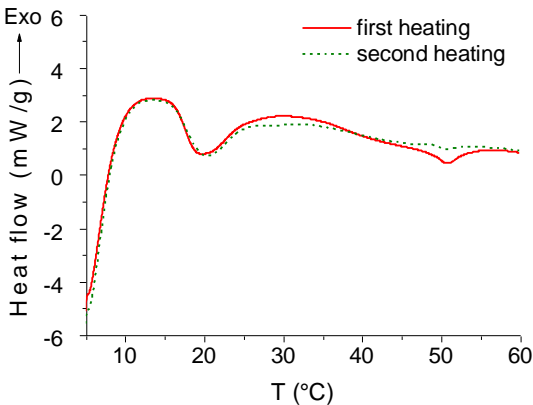
148
149 Alternative preparation with DMSO as cosolvent (DMSO/H₂O 1/2 v/v) was less challenging.
150 Gels with good mechanical strength were obtained easily by the conventional heating-cooling
151 method (see SI-8 for TEM). They were rinsed several times to remove DMSO, providing purely
152 aqueous gels. The solvent change did not alter their mechanical properties and stability, during
153 and after rinsing. However, introducing a solvent for gel formation is often undesirable, notably
154 for biocompatibility assays. For this reason, unravelling the conditions for gel formation in pure
155 water, as described above, was more challenging, but necessary.

156

157
158
159
160
161
162
163
164
165
166
167
168
169

3. Thermal transitions

The thermal transitions have been studied by DSC and by visual inspection of the sample (Figure 1). For a gel at 2wt% prepared by shearing, two transitions were observed. A first transition starting at 17°C and ending at 30°C (5 J/g with respect to the gelator; 0.2 J/g if considering the entire gel) corresponded to the loss of the macroscopic gel integrity, but large gel domains were still visible floating in a liquid phase. A second transition starting at 35°C and ending at 55°C fitted with the complete disappearance of all macroscopic gelled fragments. Over 55°C, the sample was completely liquid and clear. Both transitions were partly reversible, and the gel was recovered after 30 min at 5°C. However, repeated heating over 60°C caused the formation of a precipitate and prevented any recovery of the gel state.



170 *Figure 1. Two consecutive heating curves of hydrogel at 2wt% prepared by shearing (2°C/min).*

171

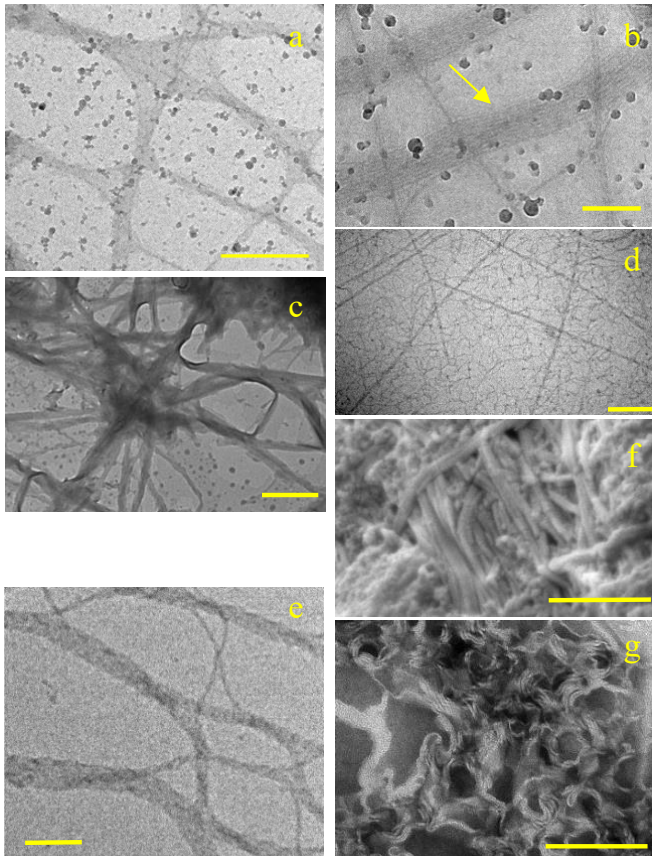
4. Morphology

The morphology of the self-assembled aggregates has been observed with different microscopic techniques and detailed by SAXS.

175

Microscopy. In a 2wt% gel obtained by shearing, two morphologies were mainly observed by TEM and cryo-TEM: intertwined helical fibres (Figure 2-e-f-g), and large and flexible ribbons or sheets (Figure 2-a-b-c). Both of them have a substructure. The wide helical fibres are made by the intertwining of thinner 10-13 nm "single" helical fibres. These 10-13 nm fibres themselves resulted from the stacking of structures with a 5-6 nm spacing. These structures are pairs of two bright bands (≈ 2.5 nm) separated by a darker one, thus can be interpreted as bilayers (Figure 2-g and SAXS). Sheets are made of long structures with 7 nm width organized in parallel side-by-side on a long range, over several millimetres (Figure 2-b). These long structures typically look like long cylindrical, wormlike micelles. Concentration played a role in the formation of the sheets. At high concentration (2wt%), sheets are the main structures observed (and confirmed by SAXS). Conversely, at lower concentration, helical fibres are the main ones. The latter are generally not able to sustain a gel. In the 2 wt% and sheared gels of Figures 2-a, b, c, helical fibres can however be seen (Figure 2-e), but they are a minority population. Shear also played a role. Without shear, the structures formed at 2wt% looked like short platelets by TEM (SI-2).

190 They are too short to sustain a intertwined network and the sample often did not gel. After shear,
 191 the intertwined long sheet-like structures are observed. These ones are able to form a persistent
 192 network throughout the sample and are able to sustain a gel. The more the sample is sheared, the
 193 more extended is this interconnected sheets structure. Besides, a population of short and
 194 randomly arranged wormlike micelles with 6-7 nm width was also observed by cryo-TEM (this
 195 population was the main one just after shearing but was still observed, to a lesser extent, after
 196 resting as well) (Figure 2-d).



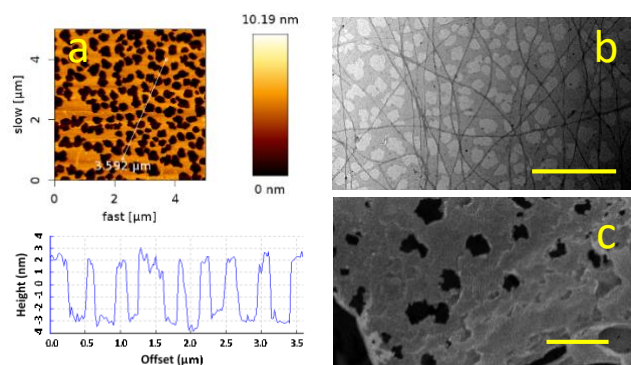
197
 198 *Figure 2. Morphologies observed in 2wt% gels in water: (a) Interconnected ribbons and flexible sheets (cryo-TEM,*
 199 *bar = 500 nm). (b) close-up within the sheet-like assemblies: ribbons of thin 7 nm fibres assembled in parallel side-*
 200 *by-side (cryo-TEM, bar = 200 nm). (c) Interconnected ribbons and flexible sheets (TEM, bar = 1 μm). (d) random*
 201 *wormlike micelles (6 nm width) observed in the background just after shearing (cryo-TEM, Bar = 200 nm). (e) single*
 202 *and intertwined 10-13 nm helical fibres (cryo-TEM, bar = 200 nm). (f) Thick twin fibres (cryo-SEM, bar = 500 nm),*
 203 *width of one single fibre = 21 nm. (g) close-up within the helical fibres revealing the twisted assembly of 5 nm thick*
 204 *structures (bilayers) (TEM, negative staining, bar = 200 nm).*

205 To better understand the effect of shear on those morphologies, cryo-TEM and TEM images
 206 were also recorded just after hydration of the solid and just after shearing. The microscopy (and
 207 also the SAXS, see below) of the solid hydrated for 16h at 2wt% in water and before shearing,
 208 already revealed the presence of 2D-sheets (Figure SI-3). Just after shearing, they were no longer
 209 observed. Instead, numerous small spots were seen on the whole grid, corresponding to dried
 210 wormlike micelles fragments (Figure SI-3). By using cryo-TEM, that avoids the formation of
 211 ambiguous drying figures, short and random 6-7 nm wide wormlike micelles were mainly
 212 observed (Figure 2-d).

213

214 The shear thus mainly broke and dispersed the sheets into individual and short wormlike
 215 micelles. After resting, these micelles re-assembled slowly into long wormlike micelles.
 216 Shearing also favoured their assembly side-by-side instead of randomly. It has been already
 217 shown that shear induced the formation of aligned wormlike micelles bundles in solutions of
 218 ionic surfactants. This association led to the formation of gels (transient or stable gels)[47].
 219 However in the case of the gels of **3**, the structures observed are much longer (more than several
 220 microns long), and are organized in 7 nm thin sheets instead of bundles. They are able to sustain
 221 a gel stable over the long term reproducibly. These structures are also reminiscent of the unusual
 222 self-assembled lamellar plaques observed by Stupp et al. for amphiphilic peptides. These plaques
 223 split under shear into bundles of parallel fibres made of long cylindrical micelles [48]. Another
 224 example of long range and flexible 2D-self-assembly leading to gelation at relatively low
 225 concentration are lamellar hydrogels. They are also quite scarce in the literature. They have a
 226 purely lamellar organisation [49],[50]. This is not the case here. Besides, samples containing
 227 mainly the intertwined 10-13 nm helical fibres often failed to gel. Probably the helical fibres
 228 entanglements do not percolate through the whole sample or are not rigid, long and persistent
 229 enough to sustain a macroscopic gelation [51].

230
 231 In contact with a surface (TEM grid), drying figures were formed. In the background of nearly
 232 all the TEM images of gelled samples, spots, but also holes with a typical jagged shape were
 233 observed (Figure 3-b). By AFM, the same jagged shapes were observed. They looked like the
 234 ones obtained for lipid bilayers dried on a surface. A constant thickness equal to 5-6 nm was
 235 measured (Figure 3-a). It matches well with the thickness of a single bilayer of gelator molecules
 236 with interdigitating alkyl chains and a polar head partly bended (Figure 5 and SI-15). Quite
 237 intriguingly, stacked layers displaying the same mosaic of jagged holes with this typical shape
 238 were observed also by cryo-SEM in addition to TEM and AFM (Figure 3-c).



239
 240 *Figure 3. Figures with "jagged holes" formed after drying. (a) bilayer membrane on mica (AFM height and profile), (b) same*
 241 *membrane pattern on TEM grid, mixed with helical fibres (bar = 2 μm) (c) same pattern in cryo-SEM (bar = 1 μm).*

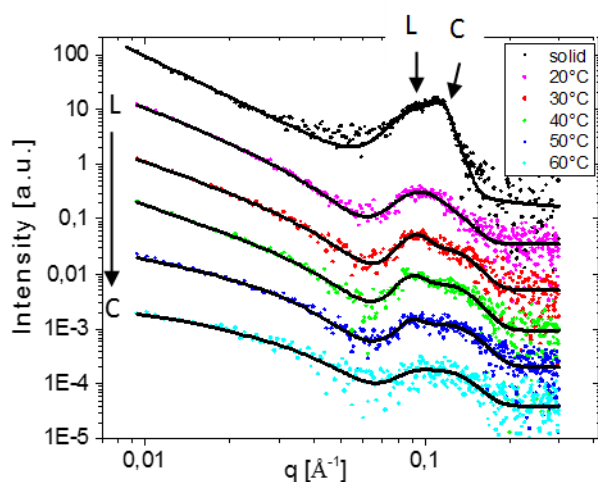
242 **Small Angle X-Ray Scattering (SAXS).** SAXS investigation was performed to detail the
 243 changes in the morphology at the nanometre scale. SAXS curves of a 2% gel from 20°C to 70°C
 244 and the one of the freeze-dried solid are shown in Figure 4. The fit results are summarized in
 245 Table 1. All curves displayed two main features as the scattering vector, q , changes: (i) a power
 246 law trend, $I(q) \propto q^{-\alpha}$, in the low q region and, (ii) a broad interaction peak in the high q region.
 247 In gel sample, at 20°C, the whole scattering curve can be described by isolated sheets with 7.1
 248 nm thickness to which two Gaussian peaks must be added in order to fully describe the high q
 249 region of the curve. These extra peaks correspond to a highly ordered state with a precise

250 correlation length very similar to a solid state. A progressive morphological change from sheets
 251 to cylinders with a diameter of about 10 nm and a length higher than 60 nm was observed from
 252 20°C to 60°C. This transition was witnessed by the change in the low q region of the curves, i.e.
 253 the power law exponent went from about 2 to 1 as the temperature increased from 20°C to 60°C
 254 (see Table 1). In this region, the exponent scales with the dimensionality proper of the scattering
 255 object. 1-D morphologies (cylinders, rods, wires, etc.) give an exponent α of 1, while 2-D
 256 morphologies (disks, lamellae, etc.) result in an exponent of 2. In general values between 1 and
 257 3 are usually associated to a mass fractal dimension where the limit of 3 is reached for full solids.
 258

259 As already said, the high q region of the scattering curves is characterized by the presence of
 260 interaction peaks. In the freeze-dried solid, these peaks were ascribed to the coexistence of two
 261 polymorphs having two different organizations, one with a 6.3 nm spacing (I1, polymorph "L",
 262 more abundant) and the other with a 5.5 nm spacing (I2, polymorph "C"). Given the flexibility
 263 of the polar head, it is very likely that the molecule can take two distinct conformations (at least)
 264 giving rise to different bilayer packings (Figure 5). In modelling, the size of a fully extended
 265 molecule is 4.2 nm (SI-15). According to the models, bilayer thicknesses should be within the
 266 range from 8.4 nm (fully extended molecule and not interdigitated) to 4.3 nm (strongly bended
 267 polar head and interdigitated).

sample	T [°C]	α	Sheet Thickness [nm]	Cylinder Radius [nm]	Cylinder Length [nm]	l_1 [nm]	l_2 [nm]
solid	20	2.7±0.1	-	-	-	6.3±0.1	5.5±0.1
hydrated solid	20	2.3±0.1	7.4±0.2	-	-	6.8±0.3	5.5±0.3
gel 2%	20	2.1±0.1	7.1±0.5	-	> 60	6.7±0.3	5.5±0.3
"	30	1.9±0.1	7.1±0.6 (0.00035)	4.9±0.3 (0.000194)	> 60	6.9±0.2	5.6±0.2
"	40	1.8±0.1	7.1±0.6 (0.00027)	4.7±0.2 (0.00023)	> 60	7.0±0.2	5.4±0.2
"	50	1.4±0.1	-	5.0±0.1	> 60	7.0±0.2	5.6±0.2
"	60	1.1±0.1	-	4.5±0.1	32±5	7.0±0.4	5.6±0.4
"	50 back	1.1±0.1	-	5.0±0.2	> 60	-	5.5±0.2
"	20 back	1.3±0.1	-	5.8±0.2	> 60	-	5.8±0.2

268
 269 *Table 1. Results of fitting of SAXS curves: dry solid, solid after 24h hydration, gel 2wt%. α = power-law index in the*
 270 *q region between 0.009 Å⁻¹ and 0.03 Å⁻¹ for gel samples and 0.009 Å⁻¹ and 0.04 Å⁻¹ for the solid; l_1 and l_2 = spacing*
 271 *distances obtained from the Gaussian interaction peaks positions from $l = 2\pi/q$ (Table SI-14-2). In brackets are*
 272 *indicated the weight of each specie in the curve fits at 30 and 40°C.*
 273

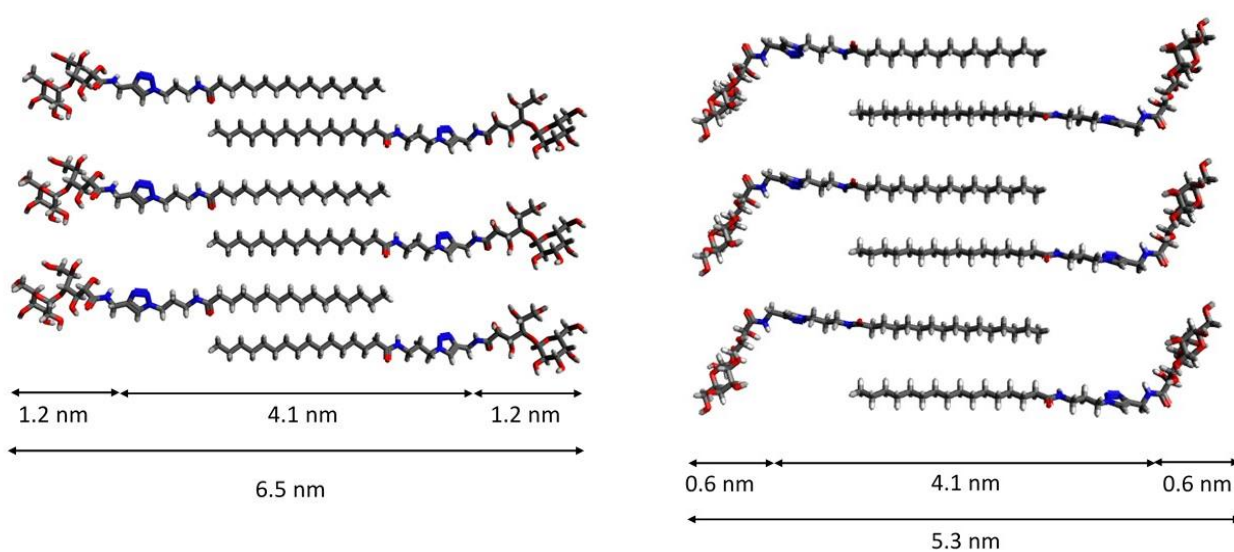


274

275 *Figure 4. SAXS curves of the freeze-dried solid at 20°C (in black, at the top) and of a 2wt% gel prepared by shearing, then*
 276 *heated from 20°C to 60°C. L = sheets. C = cylinders*

277 The dimensions measured by the interaction peaks are thus consistent with packings in which the alkyl
 278 chains are interdigitated and the polar head is more or less bended. Two examples of such packings
 279 providing a 6.5 nm (11, extended) and a 5.3 nm (12, partly bended) thickness are represented in Figure
 280 5, keeping in mind that they are only illustrative [16,37,52]. The Gaussian interaction peaks were also
 281 seen in the gel samples at 0.91 nm^{-1} and 1.14 nm^{-1} . After hydration of the solid, without shear, the
 282 interaction peaks correspond to 6.8 nm (11) and 5.5 nm (12) spacing and shearing had no main effect at
 283 this microscopic scale (SI-14-1). The shift of 11 from 6.3 nm to 6.8 nm can be attributed to the
 284 intercalation of water in inter-lamellar spaces in the gel. These interaction peaks are indicative of the
 285 presence of solid-like inhomogeneities in the gel, after hydration. We assumed that the spacing measured
 286 in these solid-like inhomogeneities is directly related to the molecular organization once the aggregates
 287 are dispersed in the solution.

288



289 *Figure 5. Illustration of possible conformations and packings of gelator 3. Up: a bilayer model with molecules in a*
 290 *fully extended conformation. Below: a bilayer model with molecules in a semi-bended conformation (molecular*
 291 *modelling suite Avogadro 1.1.1. with the Universal Force Field [53]. Colour code: C=grey, O=red, N=blue and*
 292 *H=white).*

293 From the analysis of the high q region, the ratio polymorph "L" / polymorph "C" is high in the
294 solid. Conversely, in the gel sample this ratio is drastically reduced (almost five times less). This
295 decrease is indicative of the fact that polymorph "L" in its hydrated form is more easily
296 solubilised and provides the sheet-like aggregates at 20°C. Accordingly, the dimension of
297 polymorph "L", $l_1 = 6.8-7.0$ nm, is consistent with the mean thickness of the sheets (7.1 nm).
298 And the dimension of the polymorph "C", $l_2 = 5.5$ nm, appeared to be correlated to the cylinders
299 in the gel state. Temperature did not influence much the peaks position, but it affected their ratio.
300 Actually, the weight of the peak at 1.14 nm^{-1} increased with temperature and qualitatively the
301 spectra moved at higher q values.

302
303 **Discussion.** From the results of the different experiments we concluded that after hydration,
304 mainly two kinds of self-assembled objects are formed and dispersed in the solution: assemblies
305 of cylindrical shape with a mean diameter around 10 nm (polymorph "C") and sheet-like
306 assemblies with a sheet thickness of 7.1 nm (polymorph "L"). The sheet-like assemblies are the
307 prevalent objects in solution at 20°C and in concentrated samples (2 wt%). They are the only
308 ones detectable by scattering experiments. Their size is in good agreement with the one measured
309 by cryo-TEM in the sheet-like assemblies made of long 7 nm-wide wormlike micelles,
310 assembled parallel and side-by-side (Figure 2a-b). Besides, the 10-13 nm wide helical fibres
311 found in cryo-TEM images (Figure 2e) match well the 10 nm diameter cylindrical objects
312 detected in SAXS experiments above 30°C. The diameter of these cylinders is too big to
313 correspond to cylindrical micelles. It can instead be explained by the twisting of bilayers with a
314 5-6 nm width observed by TEM (Figure 2g) and corresponding to the correlation length l_2
315 (polymorph "C") [16,36,54]. The relative ratio sheet / cylinder in the low q region of the curves
316 also decreases with temperature. The cylinders can be detected in scattering experiments only
317 above 30°C, as their concentration increases, even though a fraction already exists at room
318 temperature, as evidenced by the TEM images. The morphological transition from sheets to
319 cylinders with temperature may be induced by a change in the molecular conformation. It is
320 likely that the increase of temperature favours a bended conformation of the molecule, like in
321 the polymorph "C", more stable and characterized by a shorter molecular spacing.

322
323 These transitions agree with DSC results and macroscopic observations. In particular, in DSC
324 curves (Figure 1) a first peak at 20°C was observed, corresponding to the sheet-like structures
325 (polymorph "L"). This transition is over at 30°C. The sheet-like objects coming from the
326 polymorph "L" are responsible for the reproducible gelation after shearing, at the macroscopic
327 scale. Sheets are the main species in the 2% gel after shearing, at 20°C, but are based on weak
328 interactions. They disappear in favour of the more stable helical fibres, that exist in solution till
329 60°C. This assumption fits well with the second transition observed in DSC, at 55°C. After
330 heating the sample over 30°C, gelled fragments were still observed floating in the solution: these
331 fragments are sustained by the helical fibres. In some cases, these assemblies sustained also the
332 macroscopic gelation, even in very diluted samples (0.5 % wt or less). In those samples only the
333 transition at 55°C was observed (see SI-4). By heating up to 70°C and cooling back to 20°C,
334 only the cylinders' signature was recovered, proving that this form corresponds to a
335 thermodynamically controlled self-assembly, while the sheet-like aggregates are not. Instead
336 they are closely related to the use of shear in concentrated samples.

337

338 Another point concerning the effect of heating is shown by the SAXS curve at 20°C relative to
339 the heated sample, which failed to gel and gave a precipitate (SI-5). The curve displays an
340 interaction peak corresponding to a 4.7 nm spacing (Figure SI-14-3), that is, lower compared
341 with I1 and I2. It can correspond to a more bended conformation producing big aggregates which
342 eventually precipitate. The presence of this third polymorph "P" is observed in the interaction
343 peaks of samples once they have been cooled down from 70°C (see Figure SI-14-3, curves "50°C
344 back" and "20°C back"). The formation of a third polymorph can explain the detrimental effect
345 of heating on gel formation. This is why heating cannot be chosen as a robust protocol for
346 producing the gels in a reproducible way.

347 Besides, low concentration gels at 0.5% were obtained in a reproducible manner by diluting and
348 shearing the 2% samples. Their SAXS curves only displayed the signature of cylindrical
349 structures (see Figure SI-14-2), indicating that the sheet-like structures did not withstand
350 dilution. Using this method, the network of helical fibres produced was able to sustain the
351 formation of a macroscopic gel.

352

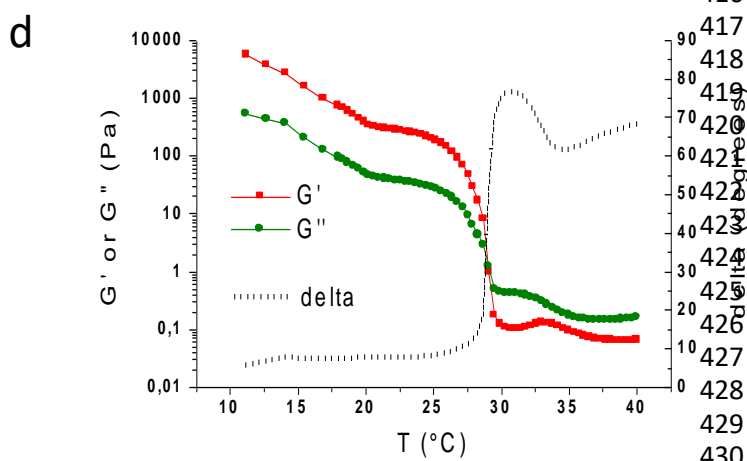
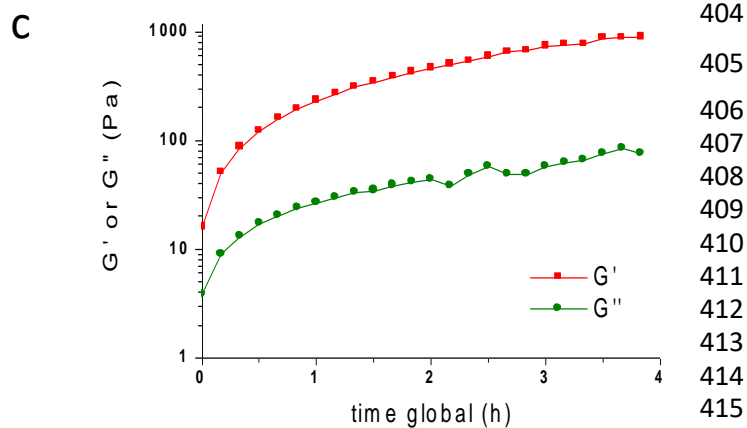
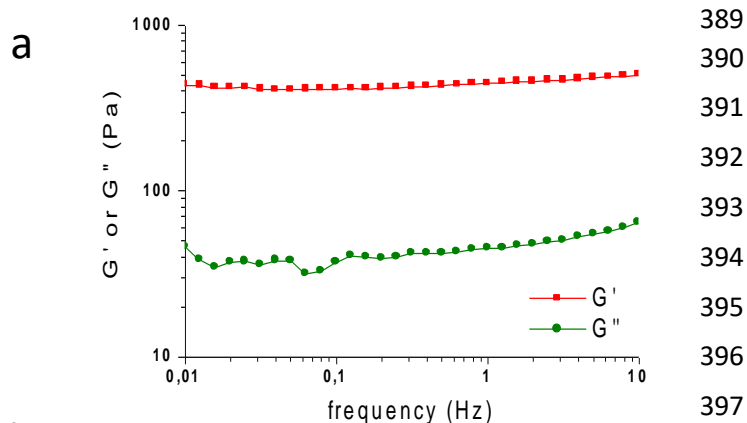
353 **E Rheology**

354 Viscoelastic and thixotropic properties of gels at 2%wt have been measured. The frequency
355 sweep from 10Hz to 0.01Hz displays a typical rheogram of gel, with $G' > G''$ over the whole
356 frequency range (Figure 6-a). G' is around 500 Pa, and G'' between 30-60 Pa, featuring a quite
357 fragile gel. The gel is thixotropic, namely after being sheared, it was able to recover its
358 viscoelastic properties after resting. This point is illustrated in Figure 6-b-c. In Figure 6b, a gel
359 ($t=0$, turned upside down) was vortexed for 15s. It flowed when turned upside down. One hour
360 later, it had recovered its gel state and did not flow when turned upside down. In Figure 6-c, a
361 gel (2%wt) was first sheared by passing through a needle, placed in the rheometer, and then G'
362 and G'' were monitored for 4h. G' in the destructured gel started at around 10Pa and progressively
363 increased as the gel restructured up to 1000 Pa. The monitoring of the gel restructuration after
364 shearing both with TEM and rheology has showed that the gel is dynamic, but with a very slow
365 rate. According to macroscopic observations, this process of gel structuration with time kept on
366 over several days and even weeks, since it was observed that some weak gels finally did not flow
367 when turned upside down far later, after several weeks. From the microscopic point of view, the
368 shear broke down the self-assembled structures formed after hydration into small objects (see
369 section D "Microscopy", Figure 2d and SI-3). These fragments coalesced back slowly, into the
370 long wormlike micelles assembled side-by-side, providing again the cross-linking points
371 sustaining the gel network.

372

373 In relation to the slow dynamics of this restructuring, interestingly, it has been shown that the
374 introduction of a sugar polar head in a dipeptide gelator (cyclo-L-Tyr-L-Lys) led to a strong
375 slowing down of the gelation process[46]. But conversely, a nucleobase-derived gelator
376 appended with a monosaccharide group displayed a quick gelation[28]. These different examples
377 raise the question on how the introduction of sugar polar heads may affect more generally the
378 self-assembly kinetics. Besides, in the case of LMW gels, thixotropy is known to be affected by
379 the nature of self-assembled structures formed (e.g. spherulites versus fibres)[55]. In our case
380 too, possibly only one of the two networks may sustain this rheological property. The
381 viscoelastic changes with temperature have also been monitored by rheology, from 10 to 40°C.
382 An abrupt decrease of the elastic modulus G' was observed from 25 to 30°C (Figure 6-d). The
383 sharp increase of the phase from 5 to 70° in this temperature range evidenced the transition from

384 a gel to a sol. The elastic (G') and viscous (G'') moduli crossed at 29°C. This measurement
 385 showed clearly the loss of the gel integrity in this range of temperature. It is consistent with the
 386 transition measured by DSC and SAXS and ascribed to the loss of the entangled sheets network
 387 of the polymorph "L".
 388



431 *Figure 6. (a) Variation of G' (elastic modulus, squares) and G'' (viscous modulus, circles) with frequency, at 1 Pa,*
432 *20°C. (b) Recovery of gel after shearing and resting for 1h. (c) Recovery of the elastic (G') and viscous (G'') modulus*
433 *with time, after shearing, measured at 0.1 Pa and 1 Hz. (d) Variation of G' , G'' and the phase (δ) with temperature,*
434 *measured at 0.8 Pa and 1 Hz.*

435

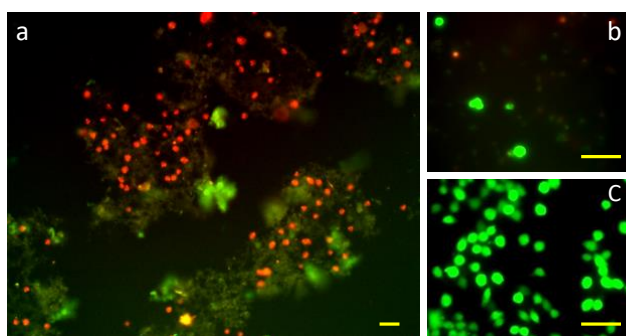
436 **F Biocompatibility**

437 Several molecular gels have been already tested as scaffold for cell culture, most of them
438 belonging to the family of gelling peptides [2,56]. Compared with polymer gels, they can provide
439 a different environment to cells, including different stiffness, a looser internal structure and
440 higher clearance, that would help cells to grow through. Injectability, related to thixotropy, is
441 also expected [2,7].

442 The gels of **3** have been tested as scaffold for cell culture with a neuronal cell line (Neuro
443 2A)[57]. After 3 days cultures, cell viability tests were performed (Figure 7). Cells adhered to
444 the gel but only a poor number of viable cells was observed (<10%) (Figure 7-b). The gels did
445 not appear suitable, whatever the method used for purifying the gelator or for preparing the gels.
446 This result is in contrast with other low molecular weight hydrogels with close chemical
447 structures on which cells were grown up to three days [58,59] or ten days [28]. Among the two
448 networks sustaining the gel, one of them was dissolved at 37°C. It may have provided a high
449 concentration of free gelator molecules, increasing the cytotoxicity. For comparison, the
450 cytotoxicity of surfactants with close structure (sugar-triazole-fatty chain) was studied in ranges
451 below 1 mmol/L, showing that surfactants with chains <6 carbons or >12 carbons had no toxicity
452 on mammalian cells in this range [60]. In our case, gels at 0.1% correspond to a concentration
453 of 1.4 mmol/L and gels at 1%, 14 mmol/L, far above the concentration range of this study. The
454 molecular gels differ strongly from polymer gels on this point, since there is no bioavailability
455 of small molecular units if biological degradation mechanisms do not provide fragments. This
456 difference in the mechanism of gelation may affect the biocompatibility.

457

458



459 *Figure 7. Cell viability assay. Neuro 2A cells have been cultured for 3 days on a 0.25%wt gel. Red staining indicates*
460 *dead cells, green staining indicates live cells. The gel also appears by green autofluorescence. Fluorescence images*
461 *at (a) low magnification and (b) high magnification. (c) Control cells after 3 days on cell culture plate. Scale bar 30*
462 *μm.*

463

464 In addition, the mechanical strength of the scaffold is known to affect the cell survival, and in
465 our gels, the dissolution of one of the two networks clearly decreased a lot the strength of the
466 gel. Accordingly, we observed that the surviving cells were exclusively aggregated on the
467 remaining gel fragments. It has been also demonstrated, in the case of amyloid peptides, that the
468 nature of the polymorph, namely the way in which the molecules self-assemble, affected the
469 cytotoxicity[40]. The same effects may occur in the case of supramolecular gelators. It points

470 out that the cell death is related not only to the chemical nature of the gel, but also to its
471 mechanical properties and to subtle molecular organisation differences.

472
473

474 **Conclusions**

475 This new sugar-based gelator, despite an easy synthetic access, displayed quite a complex
476 gelation behaviour in pure water due to polymorphism. The presence of two amides bonds, but
477 separated from each other by a rigid spacer (triazole), forces the molecule to bend and favours
478 the polymorphism. This observation may help the design of gelators. Without shearing, the
479 gelation was capricious. Starting from 2wt% solutions and applying a strong shear enabled to
480 get reproducible gelation. The resulting gels were diluted up to 0.25wt%. As a result of this
481 method, the gel was sustained by a double network, one network of thin helical fibres with 10
482 nm of diameter and an unusual network of large interconnected 2D-sheets made of thin 7 nm
483 wide wormlike micelles assembled side-by-side in parallel. The thermal transition of this second
484 network was within the room temperature range. The resulting gel was partly thermoreversible
485 and was thixotrope. Further heating, above 60°C, led to changes in the aggregation mode, giving
486 shorter aggregates which could not sustain gelation and a precipitate was formed. This work
487 illustrates that gelation can be highly dependent on the pathway used for the solubilisation and
488 the dispersion of the gelator molecules. In our case, it involved both the hydration and
489 solubilisation of the dry solid at room temperature in a range of concentration around 2wt%,
490 before shearing. This work illustrates also that full solubilisation by heating, followed by cooling
491 down can impair the self-assembly at the long range. It also showed that shearing induced the
492 formation of new self-assembled and dynamic structures able to sustain a stable gel.

493 **Acknowledgements**

494 We acknowledge the following people for their technical assistance: TEM: I. Fourquaux, D.
495 Goudounèche (CMEAB); V. Sartor, S. Gineste (IMRCP); NMR: P. Lavedan, M. Vedrenne
496 (ICT). We acknowledge the European Union for funding (AFM, DSC) (FEDER 35477: "Nano-
497 objets pour la biotechnologie") and The French National Research Agency (ANR) for financial
498 support (ANR Neuraxe). We thank the Integrated Screening Platform of Toulouse (PICT,
499 IBiSA) for providing access to HPLC equipment. LB and EF kindly acknowledge partial
500 financial support from Consorzio per lo sviluppo dei Sistemi a Grande Interfase (CSGI). Thanks
501 also to M. Mauzac for helpful discussions.

502 **References**

- 503 [1] R.G. Weiss, P. Terech, eds., *Molecular gels: materials with self-assembled fibrillar networks*,
504 Springer, Dordrecht, 2006.
- 505 [2] X. Du, J. Zhou, J. Shi, B. Xu, *Supramolecular Hydrogelators and Hydrogels: From Soft Matter*
506 *to Molecular Biomaterials*, Chem. Rev. 115 (2015) 13165–13307. doi:10.1021/acs.chemrev.5b00299.
- 507 [3] N. Zweep, J.H. van Esch, CHAPTER 1. The Design of Molecular Gelators, in: B. Escuder,
508 J.F. Miravet (Eds.), *RSC Soft Matter Ser.*, Royal Society of Chemistry, Cambridge, 2013: pp. 1–29.
509 <http://ebook.rsc.org/?DOI=10.1039/9781849737371-00001> (accessed April 4, 2016).
- 510 [4] A. Sorrenti, O. Ila, R.M. Ortuño, *Amphiphiles in aqueous solution: well beyond a soap*
511 *bubble*, Chem. Soc. Rev. 42 (2013) 8200. doi:10.1039/c3cs60151j.

512 [5] M. de Loos, B.L. Feringa, J.H. van Esch, Design and Application of Self-Assembled Low
513 Molecular Weight Hydrogels, *Eur. J. Org. Chem.* 2005 (2005) 3615–3631.
514 doi:10.1002/ejoc.200400723.

515 [6] S.S. Babu, V.K. Praveen, A. Ajayaghosh, Functional π -Gelators and Their Applications,
516 *Chem. Rev.* 114 (2014) 1973–2129.

517 [7] K.J. Skilling, F. Citossi, T.D. Bradshaw, M. Ashford, B. Kellam, M. Marlow, Insights into low
518 molecular mass organic gelators: a focus on drug delivery and tissue engineering applications, *Soft*
519 *Matter.* 10 (2014) 237–256. doi:10.1039/C3SM52244J.

520 [8] J. Raeburn, D.J. Adams, Multicomponent low molecular weight gelators, *Chem Commun.* 51
521 (2015) 5170–5180. doi:10.1039/C4CC08626K.

522 [9] D.J. Adams, P.D. Topham, Peptide conjugate hydrogelators, *Soft Matter.* 6 (2010) 3707.
523 doi:10.1039/c000813c.

524 [10] C. Tomasini, N. Castellucci, Peptides and peptidomimetics that behave as low molecular
525 weight gelators, *Chem. Soc. Rev.* 42 (2013) 156. doi:10.1039/c2cs35284b.

526 [11] K. Araki, I. Yoshikawa, Nucleobase-Containing Gelators, in: *Low Mol. Mass Gelator*,
527 Springer Berlin Heidelberg, 2005: pp. 133–165. <http://link.springer.com/chapter/10.1007/b107173>
528 (accessed January 12, 2015).

529 [12] P. Dastidar, Supramolecular gelling agents: can they be designed?, *Chem. Soc. Rev.* 37 (2008)
530 2699. doi:10.1039/b807346e.

531 [13] L.E. Buerkle, S.J. Rowan, Supramolecular gels formed from multi-component low molecular
532 weight species, *Chem. Soc. Rev.* 41 (2012) 6089. doi:10.1039/c2cs35106d.

533 [14] Y. Lin, C. Mao, Bio-inspired supramolecular self-assembly towards soft nanomaterials, *Front.*
534 *Mater. Sci.* 5 (2011) 247–265.

535 [15] N.M. Sangeetha, U. Maitra, Supramolecular gels: Functions and uses, *Chem. Soc. Rev.* 34
536 (2005) 821. doi:10.1039/b417081b.

537 [16] L.A. Estroff, A.D. Hamilton, Water gelation by small organic molecules, *Chem. Rev.* 104
538 (2004) 1201–1218.

539 [17] F. Delbecq, Supramolecular gels from lipopeptide gelators: Template improvement and
540 strategies for the in-situ preparation of inorganic nanomaterials and for the dispersion of carbon
541 nanomaterials, *Adv. Colloid Interface Sci.* 209 (2014) 98–108. doi:10.1016/j.cis.2014.02.018.

542 [18] G. Fichman, E. Gazit, Self-assembly of short peptides to form hydrogels: Design of building
543 blocks, physical properties and technological applications, *Acta Biomater.* 10 (2014) 1671–1682.
544 doi:10.1016/j.actbio.2013.08.013.

545 [19] I.W. Hamley, Lipopeptides: from self-assembly to bioactivity, *Chem Commun.* 51 (2015)
546 8574–8583. doi:10.1039/C5CC01535A.

547 [20] E.K. Johnson, D.J. Adams, P.J. Cameron, Peptide based low molecular weight gelators, *J*
548 *Mater Chem.* 21 (2011) 2024–2027. doi:10.1039/C0JM03099F.

549 [21] X.-Q. Dou, C.-L. Feng, Amino Acids and Peptide-Based Supramolecular Hydrogels for
550 Three-Dimensional Cell Culture, *Adv. Mater.* (2017) 1604062. doi:10.1002/adma.201604062.

551 [22] T.K. Lindhorst, *Essential of carbohydrate chemistry and biochemistry: [with 150 new*
552 *exercises], 3., completely rev. and enl. ed., 1. reprint, Wiley-VCH, Weinheim, 2008.*

553 [23] M.J. Clemente, R.M. Tejedor, P. Romero, J. Fitremann, L. Oriol, Maltose-based gelators
554 having azobenzene as light-sensitive unit, *RSC Adv.* 2 (2012) 11419. doi:10.1039/c2ra21506c.

555 [24] M.J. Clemente, J. Fitremann, M. Mauzac, J.L. Serrano, L. Oriol, Synthesis and
556 Characterization of Maltose-Based Amphiphiles as Supramolecular Hydrogelators, *Langmuir.* 27
557 (2011) 15236–15247. doi:10.1021/la203447e.

558 [25] M.J. Clemente, P. Romero, J.L. Serrano, J. Fitremann, L. Oriol, Supramolecular Hydrogels
559 Based on Glycoamphiphiles: Effect of the Disaccharide Polar Head, *Chem. Mater.* 24 (2012) 3847–
560 3858. doi:10.1021/cm301509v.

561 [26] M.J. Clemente, R.M. Tejedor, P. Romero, J. Fitremann, L. Oriol, Photoresponsive
562 supramolecular gels based on amphiphiles with azobenzene and maltose or polyethyleneglycol polar
563 head, *New J. Chem.* (2015). doi:10.1039/C4NJ02012J.

564 [27] G. Godeau, P. Barthélémy, Glycosyl-Nucleoside Lipids as Low-Molecular-Weight Gelators,
565 *Langmuir.* 25 (2009) 8447–8450. doi:10.1021/la900140b.

566 [28] L. Latxague, M.A. Ramin, A. Appavoo, P. Berto, M. Maisani, C. Ehret, O. Chassande, P.

567 Barthélémy, Control of Stem-Cell Behavior by Fine Tuning the Supramolecular Assemblies of Low-
568 Molecular-Weight Gelators, *Angew. Chem. Int. Ed.* 54 (2015) 4517–4521.
569 doi:10.1002/anie.201409134.

570 [29] H.P.R. Mangunuru, J.R. Yerabolu, D. Liu, G. Wang, Synthesis of a series of glucosyl triazole
571 derivatives and their self-assembling properties, *Tetrahedron Lett.* 56 (2015) 82–85.
572 doi:10.1016/j.tetlet.2014.11.013.

573 [30] E. Carretti, V. Mazzini, E. Fratini, M. Ambrosi, L. Dei, P. Baglioni, P. Lo Nostro, Structure
574 and rheology of gel nanostructures from a vitamin C-based surfactant, *Phys Chem Chem Phys.* 18
575 (2016) 8865–8873. doi:10.1039/C5CP07792C.

576 [31] A.G. Dal Bó, V. Soldi, F.C. Giacomelli, B. Jean, I. Pignot-Paintrand, R. Borsali, S. Fort, Self-
577 assembled carbohydrate-based micelles for lectin targeting, *Soft Matter.* 7 (2011) 3453.
578 doi:10.1039/c0sm01411g.

579 [32] A.G. Dal Bó, V. Soldi, F.C. Giacomelli, C. Travelet, R. Borsali, S. Fort, Synthesis,
580 micellization and lectin binding of new glycosurfactants, *Carbohydr. Res.* 397 (2014) 31–36.
581 doi:10.1016/j.carres.2014.07.021.

582 [33] G.C. Feast, T. Lepitre, X. Mulet, C.E. Conn, O.E. Hutt, G.P. Savage, C.J. Drummond, The
583 search for new amphiphiles: synthesis of a modular, high-throughput library, *Beilstein J. Org. Chem.*
584 10 (2014) 1578–1588. doi:10.3762/bjoc.10.163.

585 [34] S. Díaz-Oltra, C. Berdugo, J.F. Miravet, B. Escuder, Study of the effect of polymorphism on
586 the self-assembly and catalytic performance of an L-proline based molecular hydrogelator, *New J.*
587 *Chem.* 39 (2015) 3785–3791. doi:10.1039/C5NJ00072F.

588 [35] V.J. Nebot, S. Díaz-Oltra, J. Smets, S. Fernández Prieto, J.F. Miravet, B. Escuder, Freezing
589 Capture of Polymorphic Aggregates of Bolaamphiphilic L-Valine-Based Molecular Hydrogelators,
590 *Chem. – Eur. J.* 20 (2014) 5762–5767. doi:10.1002/chem.201400346.

591 [36] J. Cui, A. Liu, Y. Guan, J. Zheng, Z. Shen, X. Wan, Tuning the Helicity of Self-Assembled
592 Structure of a Sugar-Based Organogelator by the Proper Choice of Cooling Rate, *Langmuir.* 26 (2010)
593 3615–3622. doi:10.1021/la903064n.

594 [37] B.P. Krishnan, K.M. Sureshan, A Molecular-Level Study of Metamorphosis and
595 Strengthening of Gels by Spontaneous Polymorphic Transitions, *ChemPhysChem.* 17 (2016) 3062–
596 3067. doi:10.1002/cphc.201600590.

597 [38] S. Pan, S. Luo, S. Li, Y. Lai, Y. Geng, B. He, Z. Gu, Ultrasound accelerated gelation of novel
598 l-lysine based hydrogelators, *Chem. Commun.* 49 (2013) 8045. doi:10.1039/c3cc44767g.

599 [39] A. Baral, S. Basak, K. Basu, A. Dehsorkhi, I.W. Hamley, A. Banerjee, Time-dependent gel to
600 gel transformation of a peptide based supramolecular gelator, *Soft Matter.* 11 (2015) 4944–4951.
601 doi:10.1039/C5SM00808E.

602 [40] A.T. Petkova, Self-Propagating, Molecular-Level Polymorphism in Alzheimer’s -Amyloid
603 Fibrils, *Science.* 307 (2005) 262–265. doi:10.1126/science.1105850.

604 [41] J. Raeburn, A. Zamith Cardoso, D.J. Adams, The importance of the self-assembly process to
605 control mechanical properties of low molecular weight hydrogels, *Chem. Soc. Rev.* 42 (2013) 5143.
606 doi:10.1039/c3cs60030k.

607 [42] V.J. Nebot, D.K. Smith, CHAPTER 2. Techniques for the Characterisation of Molecular Gels,
608 in: B. Escuder, J.F. Miravet (Eds.), *RSC Soft Matter Ser.*, Royal Society of Chemistry, Cambridge,
609 2013: pp. 30–66. <http://ebook.rsc.org/?DOI=10.1039/9781849737371-00030> (accessed April 4, 2016).

610 [43] J.T. van Herpt, M.C.A. Stuart, W.R. Browne, B.L. Feringa, Mechanically Induced Gel
611 Formation, *Langmuir.* 29 (2013) 8763–8767. doi:10.1021/la401286a.

612 [44] X. Cai, Y. Wu, L. Wang, N. Yan, J. Liu, X. Fang, Y. Fang, Mechano-responsive
613 calix[4]arene-based molecular gels: agitation induced gelation and hardening, *Soft Matter.* 9 (2013)
614 5807. doi:10.1039/c3sm50577d.

615 [45] A. Reddy M, A. Srivastava, Mechano-responsive gelation of water by a short alanine-
616 derivative, *Soft Matter.* 10 (2014) 4863. doi:10.1039/c4sm00710g.

617 [46] Z. Xie, A. Zhang, L. Ye, X. Wang, Z. Feng, Shear-assisted hydrogels based on self-assembly
618 of cyclic dipeptide derivatives, *J. Mater. Chem.* 19 (2009) 6100. doi:10.1039/b912020c.

619 [47] J.J. Cardiel, A.C. Dohnalkova, N. Dubash, Y. Zhao, P. Cheung, A.Q. Shen, Microstructure
620 and rheology of a flow-induced structured phase in wormlike micellar solutions, *Proc. Natl. Acad. Sci.*
621 110 (2013) E1653–E1660. doi:10.1073/pnas.1215353110.

622 [48] S. Zhang, M.A. Greenfield, A. Mata, L.C. Palmer, R. Bitton, J.R. Mantei, C. Aparicio, M.O.
623 de la Cruz, S.I. Stupp, A self-assembly pathway to aligned monodomain gels, *Nat Mater.* 9 (2010)
624 594–601. doi:10.1038/nmat2778.

625 [49] H.E. Warriner, S.H.J. Idziak, N.L. Slack, P. Davidson, C.R. Safinya, Lamellar Biogels: Fluid-
626 Membrane-Based Hydrogels Containing Polymer Lipids, *Science.* 271 (1996) 969–973.
627 doi:10.1126/science.271.5251.969.

628 [50] J. Niu, D. Wang, H. Qin, X. Xiong, P. Tan, Y. Li, R. Liu, X. Lu, J. Wu, T. Zhang, W. Ni, J.
629 Jin, Novel polymer-free iridescent lamellar hydrogel for two-dimensional confined growth of ultrathin
630 gold membranes, *Nat. Commun.* 5 (2014). doi:10.1038/ncomms4313.

631 [51] S.R. Raghavan, J.F. Douglas, The conundrum of gel formation by molecular nanofibers,
632 wormlike micelles, and filamentous proteins: gelation without cross-links?, *Soft Matter.* 8 (2012)
633 8539. doi:10.1039/c2sm25107h.

634 [52] N. Baccile, A.-S. Cuvier, S. Prévost, C.V. Stevens, E. Delbeke, J. Berton, W. Soetaert, I.N.A.
635 Van Bogaert, S. Roelants, Self-Assembly Mechanism of pH-Responsive Glycolipids: Micelles, Fibers,
636 Vesicles, and Bilayers, *Langmuir.* 32 (2016) 10881–10894. doi:10.1021/acs.langmuir.6b02337.

637 [53] M.D. Hanwell, D.E. Curtis, D.C. Lonie, T. Vandermeersch, E. Zurek, G.R. Hutchison,
638 Avogadro: an advanced semantic chemical editor, visualization, and analysis platform, *J.*
639 *Cheminformatics.* 4 (2012) 17. doi:10.1186/1758-2946-4-17.

640 [54] L. a. Estroff, L. Leiserowitz, L. Addadi, S. Weiner, A. d. Hamilton, Characterization of an
641 Organic Hydrogel: A Cryo-Transmission Electron Microscopy and X-ray Diffraction Study, *Adv.*
642 *Mater.* 15 (2003) 38–42. doi:10.1002/adma.200390004.

643 [55] X. Huang, S.R. Raghavan, P. Terech, R.G. Weiss, Distinct Kinetic Pathways Generate
644 Organogel Networks with Contrasting Fractality and Thixotropic Properties, *J. Am. Chem. Soc.* 128
645 (2006) 15341–15352. doi:10.1021/ja0657206.

646 [56] J. Zhou, J. Li, X. Du, B. Xu, Supramolecular biofunctional materials, *Biomaterials.* 129 (2017)
647 1–27. doi:10.1016/j.biomaterials.2017.03.014.

648 [57] A. Bédou, I. Gonzales-Calvo, C. Vieu, I. Loubinoux, L. Vaysse, Investigation of the
649 Competition Between Cell/Surface and Cell/Cell Interactions During Neuronal Cell Culture on a
650 Micro-Engineered Surface, *Macromol. Biosci.* 13 (2013) 1546–1555. doi:10.1002/mabi.201300202.

651 [58] W. Wang, H. Wang, C. Ren, J. Wang, M. Tan, J. Shen, Z. Yang, P.G. Wang, L. Wang, A
652 saccharide-based supramolecular hydrogel for cell culture, *Carbohydr. Res.* 346 (2011) 1013–1017.
653 doi:10.1016/j.carres.2011.03.031.

654 [59] X. Li, Yi Kuang, J. Shi, Y. Gao, H.-C. Lin, B. Xu, Multifunctional, Biocompatible
655 Supramolecular Hydrogelators Consist Only of Nucleobase, Amino Acid, and Glycoside, *J. Am.*
656 *Chem. Soc.* 133 (2011) 17513–17518. doi:10.1021/ja208456k.

657 [60] E.D. Oldham, S. Seelam, C. Lema, R.J. Aguilera, J. Fiegel, S.E. Rankin, B.L. Knutson, H.-J.
658 Lehmler, Synthesis, surface properties, and biocompatibility of 1,2,3-triazole-containing alkyl β -d-
659 xylopyranoside surfactants, *Carbohydr. Res.* 379 (2013) 68–77. doi:10.1016/j.carres.2013.06.020.

660